JOURNAL OF VIROLOGY, Dec. 2007, p. 13259–13264
0022-538X/07/$08.00+0 doi:10.1128/JVI.01353-07

Vol. 81, No. 23

Humanized NOD/SCID/IL2Rγ^{null} Mice Transplanted with Hematopoietic Stem Cells under Nonmyeloablative Conditions Show Prolonged Life Spans and Allow Detailed Analysis of Human Immunodeficiency Virus Type 1 Pathogenesis$^{\nabla}$

Satoru Watanabe,[1,2] Shinrai Ohta,[3] Misako Yajima,[4] Kazuo Terashima,[5] Mamoru Ito,[6] Hideo Mugishima,[7] Shigeyoshi Fujiwara,[4] Kazufumi Shimizu,[2] Mitsuo Honda,[3] Norio Shimizu,[1]* and Naoki Yamamoto[3,5]*

Department of Virology, Division of Medical Science, Medical Research Institute, Tokyo Medical and Dental University, 1-5-45 Yushima, Bunkyo-ku, Tokyo 113-8519, Japan[1]; Open Research Center for Genome and Infectious Disease Control, Nihon University School of Medicine, 30-1 Oyaguchikami-chou, Itabashi-ku, Tokyo 173-8610, Japan[2]; AIDS Research Center, National Institute of Infectious Diseases, 1-23-1 Toyama, Shinjuku-ku, Tokyo 162-8640, Japan[3]; Department of Infectious Diseases, National Research Institute for Child Health and Development, 2-10-1 Okura, Setagaya-ku, Tokyo 154-8567, Japan[4]; Department of Molecular Virology, Graduate School of Medicine, Tokyo Medical and Dental University, 1-5-45 Yushima, Bunkyo-ku, Tokyo 113-8519, Japan[5]; Central Institute for Experimental Animals, 1430 Nogawa, Miyamae-ku, Kawasaki, Kanagawa 216-0001, Japan[6]; and Department of Pediatrics and Child Health, Nihon University School of Medicine, 30-1 Oyaguchikami-chou, Itabashi-ku, Tokyo 173-8610, Japan[7]

Received 21 June 2007/Accepted 3 September 2007

In a previous study, we demonstrated that humanized NOD/SCID/IL2Rγ^{null} (hNOG) mice constructed with human hematopoietic stem cells (HSCs) allow efficient human immunodeficiency virus type 1 (HIV-1) infection. However, HIV-1 infection could be monitored for only 43 days in the animals due to their short life spans. By transplanting HSCs without any myeloablation methods, the mice successfully survived longer than 300 days with stable engraftment of human cells. The mice showed high viremia state for more than the 3 months examined, with systemic HIV-1 infection and gradual decrease of CD4$^+$ T cells analogous to that in humans. These capacities of the hNOG mice are very attractive for modeling mechanisms of AIDS progression and therapeutic strategy.

One of the main problems in the field of human immunodeficiency virus type 1 (HIV-1) research is the lack of suitable small animal models for studying the virological and pathogenic aspects of human HIV-1 infection. To overcome the drawback that HIV-1 does not replicate in rodent cells, severe combined immunodeficiency (SCID) mice, engrafted with human peripheral blood mononuclear cells (hu-PBL-SCID) (16) or human fetal thymus and liver tissue [SCID-hu (Thy/Liv)] (18), have been used for the small animal models of HIV-1 infection. However, these mouse models fall short of accurately mirroring human HIV infection because of their short infection spans (17), limited infection of lymphoid tissues (15), and partial infection to coreceptor tropic HIVs (4, 10, 13).

Considering the significant advantages of developing a mouse model for HIV-1 infection, we previously introduced a novel HIV-1 mouse model using nonobese diabetic (NOD)/SCID/interleukin-2 receptor (IL-2R) gamma chain-knocked-out (NOG) mice (22). Multilineage human cells, including T, B, NK cells, monocytes/macrophages, and dendritic cells (DCs) differentiate in the mice when transplanted with human CD34$^+$ hematopoietic stem cells (HSCs) (6, 9, 22). These mice show high levels of susceptibility to both CCR5 (R5)- and CXCR4 (X4)-tropic HIVs with intense plasma viral loads lasting for over 40 days (22). Thus, this mouse model may be valuable for the study of HIV-1 infection. However, a serious problem remains. The mice showed symptoms of a wasting condition and a hunched back 5 to 7 months after HSC transplantation, following which most of them died. This life span is not sufficient if we are to better understand HIV pathogenesis and to develop novel anti-HIV countermeasures, because more than 4 months posttransplantation is required for the development of human T cells before HIV-1 can be studied in mice.

In past studies for the construction of humanized mouse models using NOD/SCID, β2 microglobulin-deficient NOD/SCID (NOD/SCID/B2m^{null}) or NOG mice, the mice were subjected to total body irradiation or given drugs for HSC transplantation (6, 9, 11, 14, 21, 23). Since NOG mice do not develop any thymic lymphomas in contrast to NOD/SCID or NOD/SCID/B2m^{null} mice (3, 19), the irradiation might influence the reduction of their life spans. In this study, we therefore searched for optimal conditions for HSC transplantation and consequently found that in NOG mice, myeloablation procedures were not required for human cell generation. Importantly, these mice stably survived

* Corresponding author. Mailing address for Naoki Yamamoto: AIDS Research Center, National Institute of Infectious Diseases, 1-23-1 Toyama, Shinjuku-ku, Tokyo 162-8640, Japan. Phone: 81-3-5285-1111. Fax: 81-3-5285-1165. E-mail: nyama@nih.go.jp. Mailing address for Norio Shimizu: Department of Virology, Division of Medical Science, Medical Research Institute, Tokyo Medical and Dental University, 1-5-45 Yushima, Bunkyo-ku, Tokyo 113-8519, Japan. Phone and fax: 81-3-5803-5811. E-mail: nshivir@tmd.ac.jp.

$^{\nabla}$ Published ahead of print on 19 September 2007.

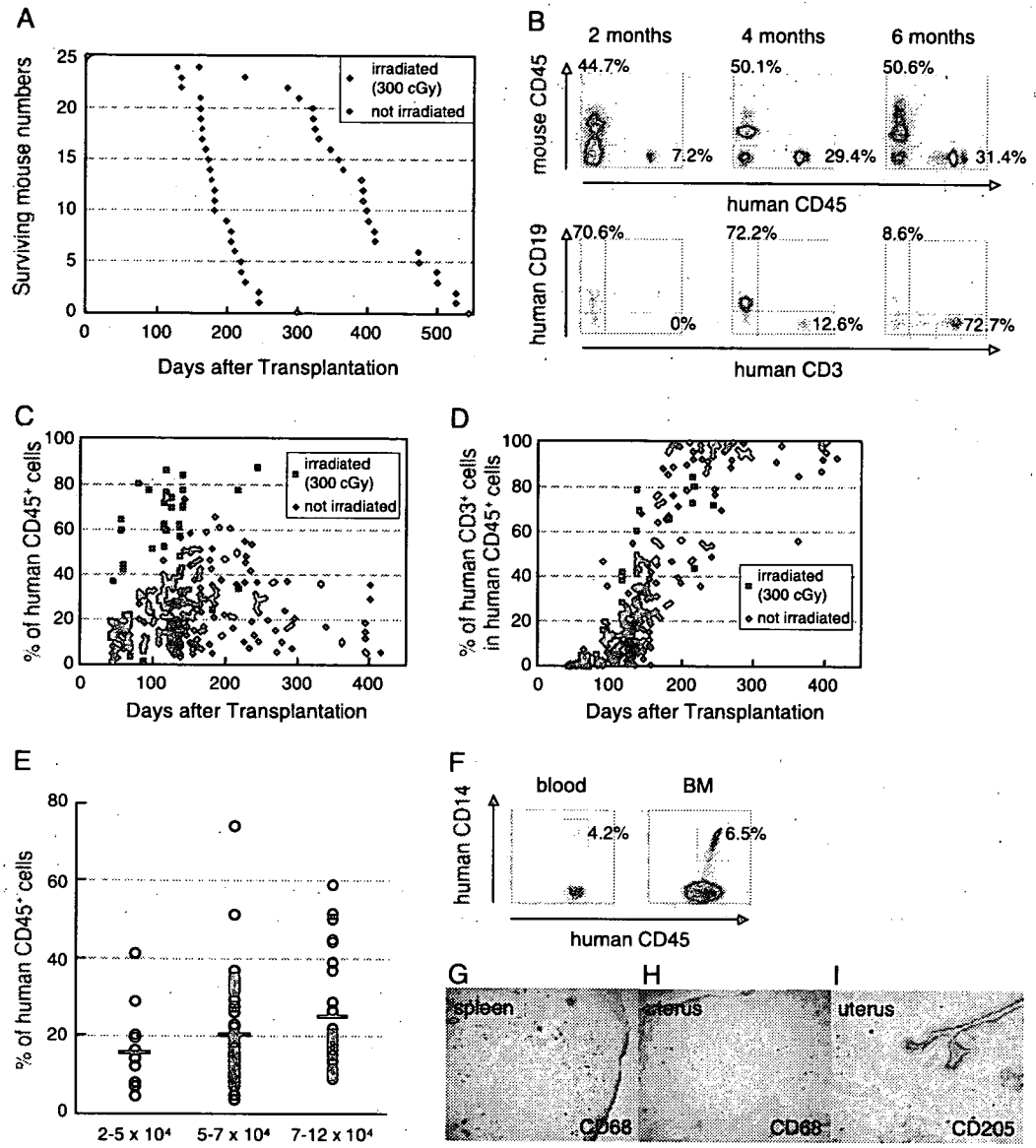

FIG. 1. Human cell generation in hematopoietic stem cell-engrafted hNOG mice with or without myeloablation. (A) Life spans of NOG mice transplanted with human stem cells after receiving 300 cGy irradiation (n = 25) or not receiving irradiation (n = 25). (B) Representative flow cytometric profiles of the mice from 2 to 6 months after transplantation without irradiation. The ratio of human to murine $CD45^+$ cells and that of human $CD3^+$ cells to $CD19^+$ cells are shown. Note that the mice generated human $CD45^+$ leukocytes that eventually developed human $CD19^+$ B cells first and then $CD3^+$ T cells. (C and D) Percentages of human $CD45^+$ cells (C) and $CD3^+$ T cells in human $CD45^+$ cells (D) in peripheral blood from 65 mice that received 300 cGy irradiation and 222 nonirradiated mice 40 to 413 days after transplantation. (E) Summary of engraftment levels in nonirradiated mice transplanted with 2×10^4 to 5×10^4 cells (n = 11), 5×10^4 to 7×10^4 cells (n = 53), or 7×10^4 to 12×10^4 (n = 30) human stem cells. Percentages of human $CD45^+$ leukocytes in peripheral blood during 4 to 5 months after transplantation were shown. The horizontal black bars indicate the averages of the groups. (F to I) Flow cytometric analysis and immunohistochemical analysis of the expression of myelomonocytic markers in nonirradiated mice 4 months after transplantation. Human $CD14^+$ monocytes/macrophages were recognized in peripheral blood and BM (F). A gate was set on the human $CD45^+$ population. Human $CD68^+$ macrophages and $CD205^+$ DCs were also detected in spleen (G) and uterus (H and I). Visualization was performed with 5-bromo-4-chloro-3-indolylphosphate (BCIP). The original magnifications were ×100 (G and H) and ×200 (I).

longer than 300 days after the HSC transplantation, which allowed further investigation of HIV-1 pathogenesis and progression to disease state in the animals.

NOG mice constructed with HSCs without myeloablation showed prolonged survival time and stable human cell generation. Six- to eight-week-old female NOG mice were obtained from the Central Institute for Experimental Animals (Kawasaki, Japan), and human cord blood-derived $CD34^+$ HSCs (2×10^4 to 12×10^4 cells) were injected intravenously with or without irradiation. As shown in Fig. 1A, most of the mice that received 300 cGy irradiation were dead within 250 days post-transplantation (mean survival time, 188 days). In contrast, more than 80% of the mice with transplanted HSCs without irradiation survived over 300 days (mean survival time, 387

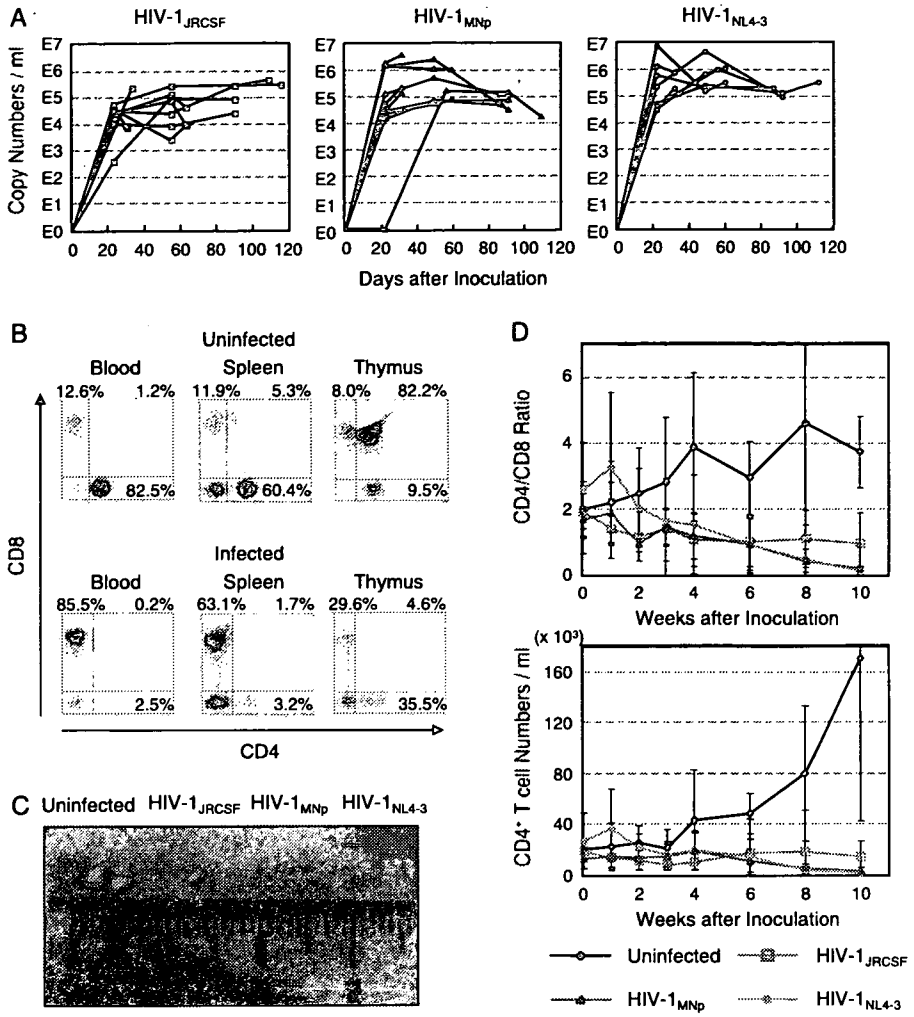

FIG. 2. Long-lasting viremia and $CD4^+$ T-cell depletion in R5- and X4-tropic HIV-1-infected hNOG mice. (A) Viral copy numbers in plasma from 29 mice intravenously inoculated with R5-tropic HIV-1_{JRCSF} (65,000 $TCID_{50}$; $n = 11$), X4-tropic HIV-1_{MNp} (20,000 $TCID_{50}$; $n = 10$), and X4-tropic HIV-1_{NL4-3} (60,000 $TCID_{50}$; $n = 8$). RNA viral copy numbers were measured using a real-time PCR quantification assay as previously described (22). (B) The percentages of $CD4^-$ $CD8^+$ (top left), $CD4^+$ $CD8^+$ (top right), and $CD4^+$ $CD8^-$ (bottom right) cells in blood, spleen, and thymus from a uninfected control mouse and a V-1_{NL4-3}-infected mouse (32 days postinfection). These two mice were constructed with HSCs from the same cord blood donor, and sacrificed 181 and 169 days after transplantation, respectively. A gate was set on the human $CD45^+$ population. (C) Comparison of the apparent size of mesenteric LN from uninfected mice or mice infected with HIV-1_{JRCSF} (109 days postinfection), HIV-1_{MNp} (109 days postinfection), or HIV-1_{NL4-3} (112 days postinfection). A uninfected control mouse was sacrificed 249 days after transplantation, and three HIV-1-infected mice were sacrificed 246, 246, and 249 days after transplantation. (D) Comparison of CD4/CD8 T-cell ratios and absolute $CD4^+$ T-cell numbers in peripheral blood from uninfected control mice ($n = 7$), R5-tropic HIV-1_{JRCSF}-infected mice ($n = 7$), X4-tropic HIV-1_{MNp}-infected mice ($n = 5$), and X4-tropic HIV-1_{NL4-3}-infected mice ($n = 6$). Results are expressed as means ± standard deviations (error bars).

days). These mice were successfully engrafted with HSCs, resulting first in the generation of human $CD19^+$ B cells and subsequently in the generation of human $CD3^+$ T cells (Fig. 1B). Figure 1C and D show the percentages of human $CD45^+$ leukocytes and human $CD3^+$ T cells in peripheral blood at 40 to 413 days after HSC transplantation. Up to 74% of leukocytes in peripheral blood samples were reconstituted with human cells in nonirradiated mice (mean ± standard deviation, 22.8% ± 14.0%; $n = 222$), and this was maintained over 400 days after transplantation (Fig. 1C). Although higher levels of human cell reconstitution were observed in the irradiated mice (45.2% ± 23.9%; $n = 65$) (Fig. 1C), which may be due to reduction of absolute numbers of murine cells by destruction of their progenitor cells in bone marrow (BM), human $CD3^+$ T cells developed with similar kinetics between the two groups (Fig. 1D). Figure 1E shows the engraftment efficiency of NOG mice transplanted with different numbers of HSCs without irradiation. More than 2×10^4 HSCs could be stably engrafted, and the levels of human cell reconstitution increased relative to the number of transplanted cells.

We further analyzed the development of human monocytes, macrophages, and DCs in the mice with transplanted HSCs without irradiation. Human $CD14^+$ monocytes were detected in peripheral blood and BM using flow cytometry (Fig. 1F), and many human $CD68^+$ macrophages were observed in various organs, including spleen (Fig. 1G), uterus (Fig. 1H), ovary, and lung (data not shown). Human $CD205^+$ DCs were also detected in spleen (data not shown) and uterus (Fig. 1I). These

TABLE 1. CD4/CD8 ratios in peripheral blood and spleen and $CD4^+$ $CD8^+$ cells in thymus of groups of uninfected and HIV-1-infected mice[a]

Group and mouse identification no.	No. of days after inoculation	CD4/CD8 ratio		% of $CD4^+$ $CD8^+$ cells in thymus	No. of RNA viral copies/ml
		Blood	Spleen		
Uninfected control group (n = 15)		2.92 ± 1.68	2.78 ± 1.46	67.8 ± 20.5	
$HIV\text{-}1_{JRCSF}$-infected group					
1	30	1.86	0.88	77.1	9,078
2	30	0.46	0.53	12.5	7,703
3	33	2.61	2.17	85.7	223,020
4	63	0.17	0.27	25.5	9,965
5	63	0.36	0.44	27.2	8,734
6	63	0.18	0.88	69.6	42,198
7	90	0.03	0.37	82.5	24,441
8	90	0.30	0.79	84.6	24,454
9	90	1.77	1.55	56.9	80,636
10	109	0.20	0.17	43.4	470,392
11	116	0.09	0.78	11.8	299,080
$HIV\text{-}1_{MNp}$-infected group					
1	31	0.82	0.44	34.6	3,709,520
2	31	1.02	0.61	90.2	219,971
3	31	1.64	1.57	78.2	135,592
4	59	0.21	0.38	35.4	78,848
5	59	0.10	0.07	77.0	1,039,716
6	87	0.20	0.40	0.5	49,080
7	87	0.19	0.08	11.7	121,817
8	91	0.04	0.04	82.9	30,706
9	91	0.28	0.10	1.2	7,407
10	109	0.00	0.21	2.8	17,310
$HIV\text{-}1_{NL4\text{-}3}$-infected group					
1	32	1.01	0.81	64.5	195,375
2	32	0.03	0.05	4.6	770,721
3	60	0.21	0.13	3.9	1,108,003
4	60	0.14	ND[b]	ND	328,375
5	87	0.03	0.04	1.0	201,207
6	92	0.03	0.17	11.1	90,831
7	92	0.03	0.03	1.4	135,514
8	112	0.30	0.23	0.2	325,202

[a] Twenty-nine mice inoculated with R5-tropic $HIV\text{-}1_{JRCSF}$ (n = 11), X4-tropic $HIV\text{-}1_{MNp}$ (n = 10), or X4-tropic $HIV\text{-}1_{NL4\text{-}3}$ (n = 8) were sacrificed 161 to 249 days after HSC transplantation. Fifteen uninfected control mice were sacrificed 174 to 249 days after transplantation, and results for the control group are expressed as means ± standard deviations.

[b] ND, not determined because of a lack of cells.

observations were similar to those seen in irradiated mice as shown in our previous report (22). Thus, humanized NOG (hNOG) mice without any myeloablation procedures allowed sufficient development of human cells to study HIV-1 pathogenesis.

hNOG mice induced systemic and long-lasting HIV-1 infection with $CD4^+$ T-cell depletion. We prepared 29 stem cell-transplanted hNOG mice and inoculated them intravenously with a high dose of R5-tropic $HIV\text{-}1_{JRCSF}$ (65,000 50% tissue culture infective doses [$TCID_{50}$]), X4-tropic $HIV\text{-}1_{MNp}$ (20,000 $TCID_{50}$), or X4-tropic $HIV\text{-}1_{NL4\text{-}3}$ (60,000 $TCID_{50}$) at 122 to 150 days posttransplantation. Then, plasma viral RNA copy numbers were measured at successive time points. The mice showed marked, long-lasting viremia state for more than 3 months, reaching the highest levels of 3.0×10^5 copies/ml from $HIV\text{-}1_{JRCSF}$-infected mice, 3.7×10^6 copies/ml from $HIV\text{-}1_{MNp}$-infected mice, and 7.8×10^6 copies/ml from $HIV\text{-}1_{NL4\text{-}3}$-infected mice (Fig. 2A). None of the mice weakened or died as a result of HIV-1 infection throughout the entire follow-up period.

All the mice were sacrificed within 4 months postinfection, and the percentages of $CD4^+$ and $CD8^+$ cells in lymphoid tissues were analyzed by flow cytometry. In a representative HIV-1-infected mouse, as shown in Fig. 2B, CD4/CD8 ratios in blood and spleen significantly decreased with apparent loss of $CD4^+$ $CD8^+$ double positive thymocytes. The size of lymphoid tissues, such as thymus and lymph node (LN), in the HIV-1-infected mice was very small compared with uninfected mice (Fig. 2C), suggesting that they shrank as a result of HIV-1 infection. Table 1 illustrates the overall profile of CD4/CD8 ratios in blood and spleen and the percentages of $CD4^+$ $CD8^+$ thymocytes from the 29 HIV-1-infected mice. Most of the mice, both R5- and X4-tropic and HIV-1 infected, had reduced CD4/CD8 ratios in blood and spleen compared with unin-

TABLE 2. Comparison of DNA proviral copies in various organs from HIV-1-infected mice[a]

Organ	No. of HIV-1 DNA copies/100 ng DNA in mice infected with[b]:		
	HIV-1_{JRCSF}	HIV-1_{MNp}	HIV-1_{NL4-3}
Peripheral blood	60	6	UD
Spleen	793	1,143	2,115
Bone marrow	2,432	656	584
Thymus	23	2,074	17,374
Lymph node	2,103	942	2,115
Lung	239	145	177
Liver	74	49	12
Small intestine	ND	6	9
Ovary	24	122	10
Uterus	14	5	16
Rectum	UD	16	11
Heart	9	UD	UD
Skin	UD	UD	138
Brain	UD	2	UD
Eyeball	3	25	UD

[a] Viral DNA was extracted from various organs of mice infected with HIV-1_{JRCSF} (33 days postinfection), HIV-1_{MNp} (59 days postinfection), and HIV-1_{NL4-3} (60 days postinfection). Determination of HIV-1 DNA copy numbers was performed by real-time PCR assay as previously described (22).

[b] UD, undetected; ND, not done.

fected control mice. On the other hand, a reduction of $CD4^+$ $CD8^+$ thymocytes was observed especially in X4-tropic HIV-1-infected mice, which seemed to correlate with the predominant expression of CXCR4 on the thymocytes as we previously described (22). Interestingly, two mice that were infected with HIV-1_{MNp} (mouse identification number 5 and 8) maintained their high percentages of $CD4^+$ $CD8^+$ thymocytes in spite of significant CD4/CD8 decline in their blood and spleen, suggesting no direct relationship between thymic T-cell depletion and CD4/CD8 decrease in peripheral blood or spleen by HIV-1 infection.

In one mouse from each R5- and X4-tropic HIV-infected group, HIV-1 proviral DNA copy numbers in various organs were measured by real-time PCR assay (Table 2). High HIV DNA copy numbers were detected in the spleen, BM, and LN of the R5-tropic HIV-1-infected mouse and in the thymus, spleen, and LN of the X4-tropic HIV-1-infected mice. In addition, HIV DNA copies were detectable in various other organs, including the lung, liver, ovary, and uterus. The fact that many human $CD68^+$ macrophages, the source of HIV-1 throughout the body (7, 8), were recognized in these organs (22) (Fig. 1H) may help explain the susceptibility of these organs to HIV-1.

To further investigate the progression of $CD4^+$ T-cell depletion by HIV-1 infection, 25 mice 120 to 151 days after HSC transplantation were randomly separated into groups of uninfected control mice (n = 7), HIV-1_{JRCSF}-inoculated mice (n = 7), HIV-1_{MNp}-inoculated mice (n = 5), and HIV-1_{NL4-3}-inoculated mice (n = 6), and then CD4/CD8 ratios and absolute $CD4^+$ T-cell numbers in peripheral blood were monitored at regular intervals. X4-tropic HIV-infected mice showed gradual decreases of their CD4/CD8 ratios and $CD4^+$ T-cell numbers, which eventually resulted in an almost complete depletion from peripheral blood (Fig. 2D). While $CD4^+$ T-cell depletion was also seen in R5-tropic HIV-infected mice, this was less prominent compared with X4-tropic HIV-1-infected mice (Fig. 2D). This pattern of R5- versus X4-tropic HIV-1 infection seems to correlate with the general observation that the emergence of X4-tropic HIVs accelerates $CD4^+$ T-cell decline and disease progression in HIV patients (12, 20).

In this study, we successfully prolonged the life span of hNOG mice by improving the HSC transplantation method and further clarified characteristics of HIV-1 infection in the mice including the following: (i) high levels of viremia lasting over 3 months, (ii) $CD4^+$ T-cell depletion in peripheral blood and spleen regardless of thymic T-cell loss, (iii) systemic HIV-1 infection not only in lymphoid tissues but also in various other organs, and (iv) a different rate of $CD4^+$ T-cell depletion for R5- versus X4-tropic HIV-1 strains. Recently, several studies on HIV-1 infection in $Rag2^{-/-}$ $\gamma c^{-/-}$ mice, transplanted with HSCs at birth, have also been reported (1, 2, 5, 24). The mice showed high susceptibility to both R5- and X4-tropic HIVs and long-term viremia with $CD4^+$ T-cell depletion, which is partly similar to our present results. However, the efficiency of human cell generation in $Rag2^{-/-}$ $\gamma c^{-/-}$ mice strongly depends on the dose of irradiation, and levels of chimerism in mice are not stable even receiving 550 to 750 cGy irradiation, which does eventually induces reduction of their life spans (5). In contrast, very stable engraftment of HSCs and subsequent human cell generation were noted in our hNOG mice even without any myeloablation procedures. Their long life spans and long-term human cell reconstitution allowed persistent HIV-1 infections mirroring HIV-1 infections in humans. Thus, this hNOG mouse system is a very useful tool as an advanced mouse model for the study of AIDS progression and long-term evaluation of new anti-HIV-1 drugs.

We thank Tomohiro Morio, Ken Watanabe, and Eiko Ogata of Tokyo Medical and Dental University for their helpful comments and skillful technical support. We are also grateful to Yukari Sasaki and Kazuhiro Takimoto of the National Institute of Infectious Diseases and Teruaki Tanaka and Junichi Fujita of the Nihon University School of Medicine for their management of animals. Human umbilical cord blood samples were obtained from the Tokyo Cord Blood Bank of the Nihon University School of Medicine.

This work was supported by a grant from the Ministry of Education, Culture, Sports, Science, and Technology to promote open research for young academics and specialists.

REFERENCES

1. **Baenziger, S., R. Tussiwand, E. Schlaepfer, L. Mazzucchelli, M. Heikenwalder, M. O. Kurrer, S. Behnke, J. Frey, A. Oxenius, H. Joller, A. Aguzzi, M. G. Manz, and R. F. Speck.** 2006. Disseminated and sustained HIV infection in $CD34^+$ cord blood cell-transplanted $Rag2^{-/-}$ $\gamma c^{-/-}$ mice. Proc. Natl. Acad. Sci. USA **103**:15951–15956.
2. **Berges, B. K., W. H. Wheat, B. E. Palmer, E. Connick, and R. Akkina.** 2006. HIV-1 infection and CD4 T cell depletion in the humanized $Rag2^{-/-}$ $\gamma c^{-/-}$ (RAG-hu) mouse model. Retrovirology **3**:76.
3. **Christianson, S. W., D. L. Greiner, R. A. Hesselton, J. H. Leif, E. J. Wagar, I. B. Schweitzer, T. V. Rajan, B. Gott, D. C. Roopenian, and L. D. Shultz.** 1997. Enhanced human $CD4^+$ T cell engraftment in beta2-microglobulin-deficient NOD-scid mice. J. Immunol. **158**:3578–3586.
4. **Fais, S., C. Lapenta, S. M. Santini, M. Spada, S. Parlato, M. Logozzi, P. Rizza, and F. Belardelli.** 1999. Human immunodeficiency virus type 1 strains R5 and X4 induce different pathogenic effects in hu-PBL-SCID mice, depending on the state of activation/differentiation of human target cells at the time of primary infection. J. Virol. **73**:6453–6459.
5. **Gorantla, S., H. Sneller, L. Walters, J. G. Sharp, S. J. Pirruccello, J. T. West, C. Wood, S. Dewhurst, H. E. Gendelman, and L. Poluektova.** 2007. Human immunodeficiency virus type 1 pathobiology studied in humanized BALB/c-$Rag2^{-/-}\gamma_c^{-/-}$ mice. J. Virol. **81**:2700–2712.
6. **Hiramatsu, H., R. Nishikomori, T. Heike, M. Ito, K. Kobayashi, K. Katamura, and T. Nakahata.** 2003. Complete reconstitution of human lym-

phocytes from cord blood CD34$^+$ cells using the NOD/SCID/γ_c^{null} mice model. Blood **102**:873–880.

7. **Igarashi, T., C. R. Brown, Y. Endo, A. Buckler-White, R. Plishka, N. Bischofberger, V. Hirsch, and M. A. Martin.** 2001. Macrophage are the principal reservoir and sustain high virus loads in rhesus macaques after the depletion of CD4$^+$ T cells by a highly pathogenic simian immunodeficiency virus/HIV type 1 chimera (SHIV): implications for HIV-1 infections of humans. Proc. Natl. Acad. Sci. USA **98**:658–663.
8. **Igarashi, T., O. K. Donau, H. Imamichi, M. J. Dumaurier, R. Sadjadpour, R. J. Plishka, A. Buckler-White, C. Buckler, A. F. Suffredini, H. C. Lane, J. P. Moore, and M. A. Martin.** 2003. Macrophage-tropic simian/human immunodeficiency virus chimeras use CXCR4, not CCR5, for infections of rhesus macaque peripheral blood mononuclear cells and alveolar macrophages. J. Virol. **77**:13042–13052.
9. **Ito, M., H. Hiramatsu, K. Kobayashi, K. Suzue, M. Kawahata, K. Hioki, Y. Ueyama, Y. Koyanagi, K. Sugamura, K. Tsuji, T. Heike, and T. Nakahata.** 2002. NOD/SCID/γ_c^{null} mouse: an excellent recipient mouse model for engraftment of human cells. Blood **100**:3175–3182.
10. **Kaneshima, H., L. Su, M. L. Bonyhadi, R. I. Connor, D. D. Ho, and J. M. McCune.** 1994. Rapid-high, syncytium-inducing isolates of human immunodeficiency virus type 1 induce cytopathicity in the human thymus of the SCID-hu mouse. J. Virol. **68**:8188–8192.
11. **Kollet, O., A. Peled, T. Byk, H. Ben-Hur, D. Greiner, L. Shultz, and T. Lapidot.** 2000. β2 Microglobulin-deficient (B2m^{null}) NOD/SCID mice are excellent recipients for studying human stem cell function. Blood **95**:3102–3105.
12. **Koot, M., I. P. Keet, A. H. Vos, R. E. de Goede, M. T. Roos, R. A. Coutinho, F. Miedema, P. T. Schellekens, and M. Tersmette.** 1993. Prognostic value of HIV-1 syncytium-inducing phenotype for rate of CD4$^+$ cell depletion and progression to AIDS. Ann. Intern. Med. **118**:681–688.
13. **Koyanagi, Y., Y. Tanaka, J. Kira, M. Ito, K. Hioki, N. Misawa, Y. Kawano, K. Yamasaki, R. Tanaka, Y. Suzuki, Y. Ueyama, E. Terada, T. Tanaka, M. Miyasaka, T. Kobayashi, Y. Kumazawa, and N. Yamamoto.** 1997. Primary human immunodeficiency virus type 1 viremia and central nervous system invasion in a novel hu-PBL-immunodeficient mouse strain. J. Virol. **71**:2417–2424.
14. **Matsumura, T., Y. Kametani, K. Ando, Y. Hirano, I. Katano, R. Ito, M. Shiina, H. Tsukamoto, Y. Saito, Y. Tokuda, S. Kato, M. Ito, K. Motoyoshi, and S. Habu.** 2003. Functional CD5$^+$ B cells develop predominantly in the spleen of NOD/SCID/γc^{null} (NOG) mice transplanted either with human umbilical cord blood, bone marrow, or mobilized peripheral blood CD34$^+$ cells. Exp. Hematol. **31**:789–797.
15. **McCune, J., H. Kaneshima, J. Krowka, R. Namikawa, H. Outzen, B. Peault, L. Rabin, C. C. Shih, E. Yee, M. Lieberman, I. Weissman, and L. Shultz.** 1991. The SCID-hu mouse: a small animal model for HIV infection and pathogenesis. Annu. Rev. Immunol. **9**:399–429.
16. **Mosier, D. E., R. J. Gulizia, S. M. Baird, D. B. Wilson, D. H. Spector, and S. A. Spector.** 1991. Human immunodeficiency virus infection of human-PBL-SCID mice. Science **251**:791–794.
17. **Mosier, D. E., R. J. Gulizia, P. D. MacIsaac, B. E. Torbett, and J. A. Levy.** 1993. Rapid loss of CD4$^+$ T cells in human-PBL-SCID mice by noncytopathic HIV isolates. Science **260**:689–692.
18. **Namikawa, R., H. Kaneshima, M. Lieberman, I. L. Weissman, and J. M. McCune.** 1988. Infection of the SCID-hu mouse by HIV-1. Science **242**:1684–1686.
19. **Shultz, L. D., P. A. Schweitzer, S. W. Christianson, B. Gott, I. B. Schweitzer, B. Tennent, S. McKenna, L. Mobraaten, T. V. Rajan, D. L. Greiner, et al.** 1995. Multiple defects in innate and adaptive immunologic function in NOD/LtSz-scid mice. J. Immunol. **154**:180–191.
20. **Tersmette, M., R. A. Gruters, F. de Wolf, R. E. de Goede, J. M. Lange, P. T. Schellekens, J. Goudsmit, H. G. Huisman, and F. Miedema.** 1989. Evidence for a role of virulent human immunodeficiency virus (HIV) variants in the pathogenesis of acquired immunodeficiency syndrome: studies on sequential HIV isolates. J. Virol. **63**:2118–2125.
21. **Ueda, T., H. Yoshino, K. Kobayashi, M. Kawahata, Y. Ebihara, M. Ito, S. Asano, T. Nakahata, and K. Tsuji.** 2000. Hematopoietic repopulating ability of cord blood CD34$^+$ cells in NOD/Shi-*scid* mice. Stem Cells **18**:204–213.
22. **Watanabe, S., K. Terashima, S. Ohta, S. Horibata, M. Yajima, Y. Shiozawa, M. Z. Dewan, Z. Yu, M. Ito, T. Morio, N. Shimizu, M. Honda, and N. Yamamoto.** 2007. Hematopoietic stem cell-engrafted NOD/SCID/IL2Rγ^{null} mice develop human lymphoid systems and induce long-lasting HIV-1 infection with specific humoral immune responses. Blood **109**:212–218.
23. **Yahata, T., K. Ando, Y. Nakamura, Y. Ueyama, K. Shimamura, N. Tamaoki, S. Kato, and T. Hotta.** 2002. Functional human T lymphocyte development from cord blood CD34$^+$ cells in nonobese diabetic/Shi-*scid*, IL-2 receptor γ null mice. J. Immunol. **169**:204–209.
24. **Zhang, L., G. I. Kovalev, and L. Su.** 2007. HIV-1 infection and pathogenesis in a novel humanized mouse model. Blood **109**:2978–2981.

Int Ophthalmol (2007) 27:383–386
DOI 10.1007/s10792-007-9090-5

CASE REPORT

Kinetics of aqueous flare, intraocular pressure and virus-DNA copies in a patient with cytomegalovirus iridocyclitis without retinitis

Tatsushi Kawaguchi · Sunao Sugita · Norio Shimizu · Manabu Mochizuki

Received: 4 December 2006 / Accepted: 12 April 2007 / Published online: 24 May 2007

Abstract
Background A case report of recurrent unilateral granulomatous iridocyclitis with ocular hypertension without retinitis caused by cytomegalovirus (CMV) in an immunocompetent patient.
Methods Aqueous humor was analysed by multiplex PCR to detect viral DNA, and real-time PCR was used to evaluate virus copies before and after anti-virus treatments. Inflammation of the anterior chamber was evaluated by a laser flare photometry.
Results Genomic DNA of CMV – but not of other herpes viruses – was detected in the aqueous humor. Quantitative real-time PCR revealed 2.3×10^5 copies/ml of CMV DNA from the specimen. Oral valganciclovir was added to the ongoing treatment, which consisted of topical corticosteroid, timolol and latanoprost as well as systemic acetazolamide, resulting in the reduction of aqueous flare correlated with the reduction of virus copies in aqueous humor.
Conclusions In this case of CMV-related iridocyclitis in an immunocompetent patient, specific additional anti-viral therapy was effective in controlling inflammation of anterior chamber but, as is so often the case, it was unable to control intraocular pressure. We show that inflammatory activity correlated well with the number of virus copies in the aqueous humor.

Keywords Cytomegalovirus · Iridocyclitis

T. Kawaguchi (✉) · S. Sugita · M. Mochizuki
Department of Ophthalmology & Visual Science, Tokyo Medical and Dental University Graduate School of Medicine, 1-5-45 Yushima, Bunkyo-ku, Tokyo 113-8519, Japan
e-mail: kouseidon2002@yahoo.co.jp

N. Shimizu
Department of Virology, Medical Research Institute, Tokyo Medical and Dental University Graduate School of Medicine, Tokyo, Japan

Introduction

Cytomegalovirus (CMV), a member of the herpes virus family, is known to be a common cause of necrotic retinitis in immunocompromised hosts [1]. CMV infection does not usually cause clinically noticeable disease in healthy individuals, but congenitally infected infants and immunosuppressed individuals, such as patients with acquired immunodeficiency syndrome (AIDS), can develop severe sight-threatening disease.

Several recently published articles have reported CMV-related anterior uveitis unassociated with necrotic retinitis in immunocompetent individuals [2–4]. We report here a patient in whom the presence of CMV DNA was confirmed by PCR analysis of aqueous humor from the eye with recurrent iridocyclitis without posterior involvement; the number of virus copies correlated well with the aqueous flare.

Case report

A 66-year-old man was referred to the uveitis clinic at Tokyo Medical and Dental University Hospital in July 2005 because of elevated intraocular pressure (IOP) – up to 30 mmHg in the right eye – associated with recurrent iridocyclitis. He had been considered a case of Posner-Schlossman syndrome for 8 years and treated with topical corticosteroid, timolol, latanoprost and dorzolamide. On the initial presentation to our clinic, his visual acuity was 0.8 in the right eye (RE) and 1.2 in the left eye. Examination of the RE revealed the presence of whitish, small, mutton-fat keratic precipitates and mild inflammation in the anterior chamber. The pigmentation of the trabecular meshwork in the affected eye was much less intense than that of the normal left eye and there were no posterior synechiae (Fig. 1). Iris atrophy and iris depigmentation were absent in the RE as was retinitis and vitreous opacity. There were no abnormal findings in the left eye.

Systemic investigations and laboratory tests revealed no systemic disease, and serology for human immunodeficiency virus (HIV) was negative. Serum IgG and IgM antibodies against herpes simplex virus (HSV) were negative, whereas IgG titers against varicella-zoster virus (VZV) and cytomegalovirus (CMV) were positive. After informed consent was obtained, an aliquot (100 μl) of aqueous humor was obtained from the anterior chamber of the RE. DNA was extracted from the aqueous humor sample using a DNA minikit (Qiagen, Valencia, Calif.). Multiplex PCR was performed using a LightCycler (Roche, Switzerland). The primers of the glycoprotein gene sequences for CMV were TACCCCTATCGCGTG TGTTC (forward) and ATAGGAGGCGCCACGTATTC (reverse); the probes were 3′-FITC-TCGTCGTAGCTACGCTTACAT and LcRed705-5′-ACACCACTTATCTGCTGGGCAGC. The specific primers for the virus were used with Accuprim *Taq* (Invitrogen, Carlsbad, Calif.). The PCR amplification conditions were as reported previously [5]. Multiplex PCR analyses of the sample revealed the presence of genomic DNA of CMV but not of genomic DNA of other herpes viruses (HSV-1, HSV-2, VZV, EBV, HHV-6, HHV-7 and HHV-8). Real-time PCR was performed using Amplitaq Gold and the Real-Time PCR 7300 system (ABI, Forster City, Calif.). The primers of the gene sequences and the PCR amplification conditions were as reported previously by Griscelli et al. [6]. Quantitative real-time PCR revealed 2.3×10^5 copies/ml of CMV-DNA from the specimen.

Based on the clinical findings and PCR results, we made the diagnosis of iridocyclitis with ocular hypertension caused by CMV and commenced treatment with systemic valganciclovir (1800 mg/day) in addition to ongoing topical steroid and antiglaucomatous drugs. The intensity of anterior uveitis measured by laser flare photometry (model FC1000; KOWA, Japan) decreased following the treatment (Fig. 2). In addition, the clinical course of the anterior uveitis correlated well with the CMV-DNA copies in the aqueous humor, as measured on samples taken at the time of surgical interventions. However, intraocular pressure was not controlled by the medication and often evolved in an inverse, yet proportional manner to the inflammation. Trabeculectomy had to be performed to the RE, and CMV-DNA was detected in the aqueous humor obtained at the time of operation (1.1×10^4 copies/ml). DNA was also extracted from the samples of iris tissue

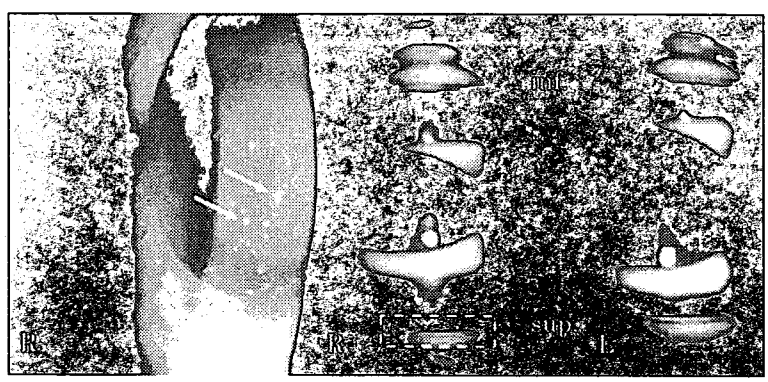

Fig. 1 Slitlamp findings of anterior segment. **Left panel** Multiple middle-sized white-gray precipitates presented in the central cornea (*arrows*). **Right panel** Gonioscopy showed less pigmentation at a chamber angle in the right eye (*area within the white broken line*)

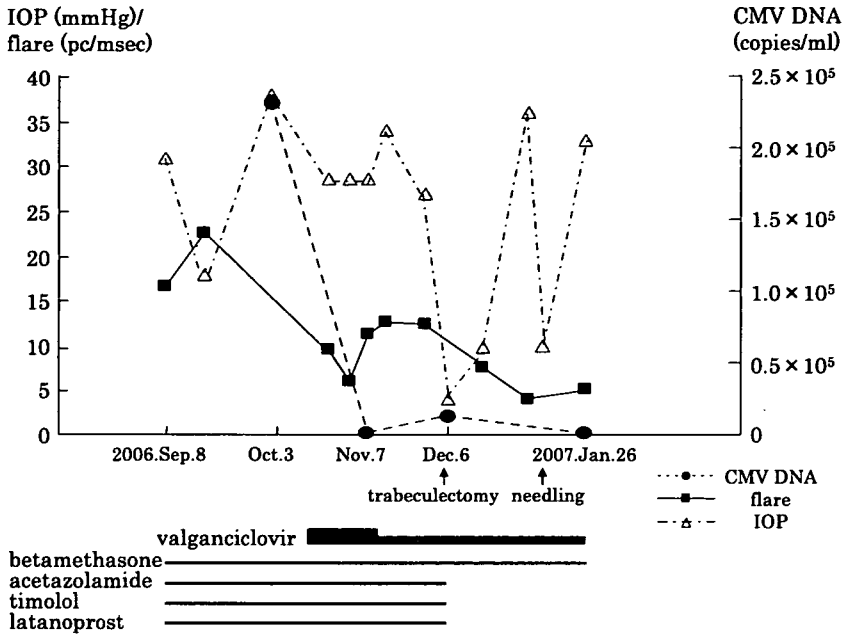

Fig. 2 Prognosis of cytomegalovirus (*CMV*) DNA copies, aqueous flare and intraocular pressure (*IOP*). Aqueous flare was reduced following the anti-CMV treatment in direct correlation with the number of virus copies

and trabecular meshwork tissue by DNeasy tissue kit (QIAGEN). However, genomic DNA of CMV was not detected in the sample from the iris and trabecular meshwork.

Discussion

CMV has been believed to rarely cause ocular involvement in healthy adults. However, Mietz et al. reported the local production of anti-CMV antibodies from the aqueous humor in patients with iridocyclitis concomitant with glaucoma [2]. Markomichelakis et al. reported two cases of iridocyclitis with sectoral iris atrophy in which PCR testing was positive for CMV but negative for HSV and VZV [3]. Schryver et al. described five cases of iridocyclitis related to CMV infection that were similar those reported elsewhere [4]. Koizumi et al. recently reported the presence of CMV DNA in the aqueous humor of a patient with corneal endotheliitis without immunodepression [7]. In all of these reports, specific anti-CMV therapy, mostly systemic ganciclovir, was effective against not only anterior chamber inflammation but also high intraocular pressure.

To the best of our knowledge, this is the first case report that describes the correlation between viral load of CMV and inflammatory flare in the aqueous humor. In our case, oral valganciclovir was effective in reducing both the number of virus copies in the aqueous humor and anterior chamber inflammation. These results indicate that CMV infection can cause recurrent iridocyclitis in immunocompetent patients. In contrast to previous reports, intraocular pressure in our patient did not respond to anti-CMV therapy, even though genomic DNA of CMV was not detected in the trabecular meshwork. The trabecular meshwork in the affected eye may have been destroyed and have irreversibly lost the filtrating function or long-term usage of topical corticosteroid may be one factor at the origin of ocular hypertension. We do not know why genomic DNA of CMV was not detectable in the iris and trabecular meshwork. However, we examined only the limited amount of tissues obtained from the surgery and not the whole tissues. This could be one reason that explains the discrepancy between the aqueous humor and these tissues obtained from this patient.

The high CMV viral load in this patient is significant in that its presence in the aqueous humor suggests that CMV may play a direct pathogenic role in the anterior segment inflammation. Another possibility is that long-term usage of topical corticosteroid may have created a steroid reservoir, resulting in an immunosuppressed local anterior segment that enabled CMV replication. However, this is pure

speculation, and additional patients will be needed to confirm such a hypothesis.

The present case had clinical features similar to Posner-Schlossman syndrome (PSS), i.e. unilateral anterior uveitis characterized by small, whitish keratic precipitates and mild inflammation in the anterior chamber with high ocular tension together with depigmentation of trabecular meshwork in the affected eye [8]. Bloch-Michel et al. reported the local production of anti-CMV antibodies in the aqueous humor in a patient with PSS, suggesting a relation between PSS and CMV infection [9]. In fact, the present patient was followed as PSS for 8 years. The data reported by Bloch-Michel et al. [9] together with the data on our patient suggest that, in future, patients with PSS might increasingly be examined for an association to CMV infection. The clinical implication may be that patients with PSS should only be considered as such once CMV infection of the anterior segment has been excluded. Virological tests on an ocular specimen, especially the PCR assay on aqueous humor, are considered to be essential for an early and accurate diagnosis.

Acknowledgements We greatly appreciate Dr. Tomohiro Morio for advising and testing the real-time PCR. We thankDrs. Yuri Futagami, Shintaro Horie, Ken Watanabe and Miki Mizukami for their technical assistance. The authors also appreciate Dr. Carl P. Herbort for his valuable discussion and comments. Partial financial support from Grant-in-Aid for Young Scientists (B) 18791263 of the Ministry of Education, Culture, Sports and Technology, Japan.

References

1. Yoser SL, Forster DJ, Rao NA (1993) Systemic viral infections and their retinal and choroidal manifestations. Surv Ophthalmol 37:313–352
2. Mietz H, Aisenbrey S, Bartz-Schmidt KU, Bamborshke S, Krieglstein G (2000) Ganciclovir for the treatment of anterior uveitis. Graefe's Arch Clin Exp Ophthalmol 238:905–909
3. Markomichelakis NM, Canakis C, Zafirakis P, Marakis T, Mallias I, Theodossiadis G (2002) Cytomegalovirus as a cause of anterior uveitis with sectoral iris atrophy. Ophthalmology 109:879–882
4. Schryver I, Rozenberg F, Cassoux N, Michelson S, Kestelyn P, Davis JL, Bodaghi B (2006) Diagnosis and treatment of cytomegalovirus iridocyclitis without retinal necrosis. Br J Ophthalmol 90:852–855
5. Schaade L, Kockelkorn P, Ritter K, Kleines M (2000) Detection of cytomegalovirus DNA in human specimens by LightCycler. J Clin Microbiol 38:4006–4009
6. Griscelli F, Barrois M, Chauvin S, Lastere S, Bellet D, Bourhis JH (2001) Quantification of human cytomegalovirus DNA in bone marrow transplant recipients by real-time PCR. J Clin Microbiol. 39:4362–4369
7. Koizumi N, Yamasaki K, Kawasaki S, Sotozono C, Inatomi T, Mochida C, Kinoshita S (2006) Cytomegalovirus in aqueous humor from an eye with corneal endotheliitis. Am J Ophthalmol 141: 564–565
8. Posner A, Schlossman A (1948) Syndrome of unilateral recurrent attacks of glaucoma with cyclitic symptoms. Arch Ophthalmol 39:517–528
9. Bloch-Michel E, Dussaix E, Cerqueti P, Patarin D (1987) Possible role of cytomegalovirus infection in the etiology of the Posner-Schlossman syndrome. Int Ophthalmol 11:95–96